Biochemical Engineering Journal 207 (2024) 109333

Contents lists available at ScienceDirect

Biochemical Engineering Journal

journal homepage: www.elsevier.com/locate/bej

Regular article

Intensification of a biocatalytic oxidation under fine bubble aeration in a rotating bed reactor

Zeynep Perçin [a], Lotta Kursula [b], Erik Löfgren [c], Emil Byström [c], Felix Kexel [b], Paul Bubenheim [a], Michael Schlüter [b], Andreas Liese [a,*]

[a] Institute of Technical Biocatalysis, Denickestr, 15, Hamburg, Hamburg 21073, Germany
[b] Institute of Multiphase Flows, Eißendorfer Str, 38, Hamburg, Hamburg 21073, Germany
[c] SpinChem AB, Tvistevägen 48C, Umeå 90736, Sweden

ARTICLE INFO

Keywords:
Process optimization/validation
Microbubble aeration
Repetitive batch
Covalent immobilization
Sustainability

ABSTRACT

The utilization of oxidases suffers from insufficient oxygen availability due to its low solubility in gas-liquid multiphase systems. To overcome this limitation, oxygen is continuously supplied to the reaction medium during the course of the reaction, however, it causes significant gas consumption. In this study, a novel experimental set-up was established by installing a sintered frit porous sparger in the SpinChem® rotating bed reactor. Covalently immobilized glucose oxidase on epoxy-functionalized carriers was used in the rotating bed reactor with an activity yield of the immobilization of over 98%. For fine bubble aeration, the volumetric mass transfer coefficient k_La (67.3 h^{-1}) tripled compared to macrobubble aeration (22.5 h^{-1}), while the volume-specific aeration rate remained constant. A maximum reaction yield of 96.5% was reached. The reaction rate was improved by a factor of 12.9 for the fine bubble aeration compared to macrobubble aeration under identical conditions. With fine bubble aeration, the oxygen consumption was reduced by 87.5% over macrobubble aeration, establishing the same enzyme-specific reaction rates at a comparable k_La. Validation was carried out in repetitive batches, achieving the same glucose oxidase specific activity. This study demonstrates the advantages of fine bubble aeration and presents promising results for addressing the sustainable biotransformation processes.

1. Introduction

The production of chemicals using biocatalytic reactions, which utilize gaseous substrates is of increasing importance [1,2]. One of the major challenges in biocatalytic oxidative processes catalyzed by oxidases is the low oxygen solubility (0.254 mM at 1 atm and 25 °C in water [3]) in gas–liquid multiphase systems [4,5]. Therefore, a high mass transfer of molecular oxygen into the bulk medium is necessary to oxidize high substrate concentrations in a reasonable process time. Many studies have been conducted to optimize biocatalytic processes with different approaches, including reactor concepts intensified with flow biocatalysis operating under atmospheric and high pressure conditions [6–9].

To overcome the limitation of inadequate availability of a gaseous substrate, well-mixed conditions are ensured to minimize inhomogeneities and achieve efficient gas-liquid mass transfer. The mass transfer performance was improved by either increasing the pressure [9] or by increasing the surface area per volume of gas available for mass transfer at the gas-liquid interphase, as shown in our previous studies [10–12], where the sintered frit porous spargers were used to generate fine bubbles. In accordance with ISO 20480, fine bubbles are subdivided into ultrafine bubbles ($d < 1$ μm) and microbubbles (1 μm $\leq d <$ 100 μm) [13], with microbubbles being of interest in this study. For fine bubbles, the effect of buoyancy becomes less dominant, and the rising velocity of the bubbles decreases with a smaller diameter [14]. This results in a longer residence time of the bubbles and thus a higher mass transfer into the reaction medium. Furthermore, for fine bubbles, the Laplace pressure increases significantly leading to a higher partial pressure inside the bubble [11,14,15]. Therefore, the concentration gradient at the interphase is increased with a lower bubble diameter in accordance with Henry's law leading to locally increased saturation concentrations [14,16].

In this study, molecular oxygen dissolved in the reaction medium is used as a second substrate in the biocatalytic oxidation of glucose by the immobilized enzyme glucose oxidase (GOx). Fine bubbles containing oxygen provide a larger volume-specific surface area, resulting in a

* Corresponding author.
E-mail address: liese@tuhh.de (A. Liese).

https://doi.org/10.1016/j.bej.2024.109333
Received 19 February 2024; Received in revised form 10 April 2024; Accepted 13 April 2024
Available online 15 April 2024

higher volumetric mass transfer coefficient [10–12]. According to S. Illner, the increase in surface area to volume ratio improves the contact between the gas and liquid phases for the reaction catalyzed by the enzyme GOx in solubilized form, thus achieving a higher space-time yield [17]. In this work, the SpinChem® rotating bed reactor (RBR) integrated with a sintered frit porous sparger with a pore diameter of 2 μm was used as an alternative to conventional packed bed reactors. The SpinChem® RBR S2 acts as an impeller in the form of a rotating basket (diameter 45 mm) inserted into the SpinChem® vessel V2. The reactants, together with air bubbles containing oxygen, are distributed in the liquid medium [18]. The reaction medium, including oxygen within fine bubbles, is partially passed through the RBR, where the model reaction is catalyzed by covalently immobilized GOx on epoxy-functionalized carriers, and is discharged back to the vessel (depicted in Fig. 1). The hydrodynamic characterization of the resulting radial flow pattern is under investigation. In addition, the reusability of enzymes is considered for an economical process and enzyme immobilization is a useful method to enable the reuse of biocatalysts [19]. The RBR is fully packed with carriers, on which enzymes are covalently immobilized to carry out the model reaction (shown in Scheme 1). Our study demonstrates the applicability of fine bubble aeration in the RBR filled with immobilized catalyst as an efficient novel reactor design for process intensification.

2. Material and methods

2.1. Biocatalysis

Glucose oxidase (Enzyme Commission Number: 1.1.3.4) GOx type VII (G2133) lyophilized powder from *Aspergillus niger* and peroxidase (Enzyme Commission Number: 1.11.1.7) type I (P8125) lyophilized powder from horseradish were purchased from Sigma-Aldrich/Merck KGaA (Germany). Catalase (Enzyme Commission Number: 1.11.1.6) (C0052) solid powder from bovine liver was purchased from TCI

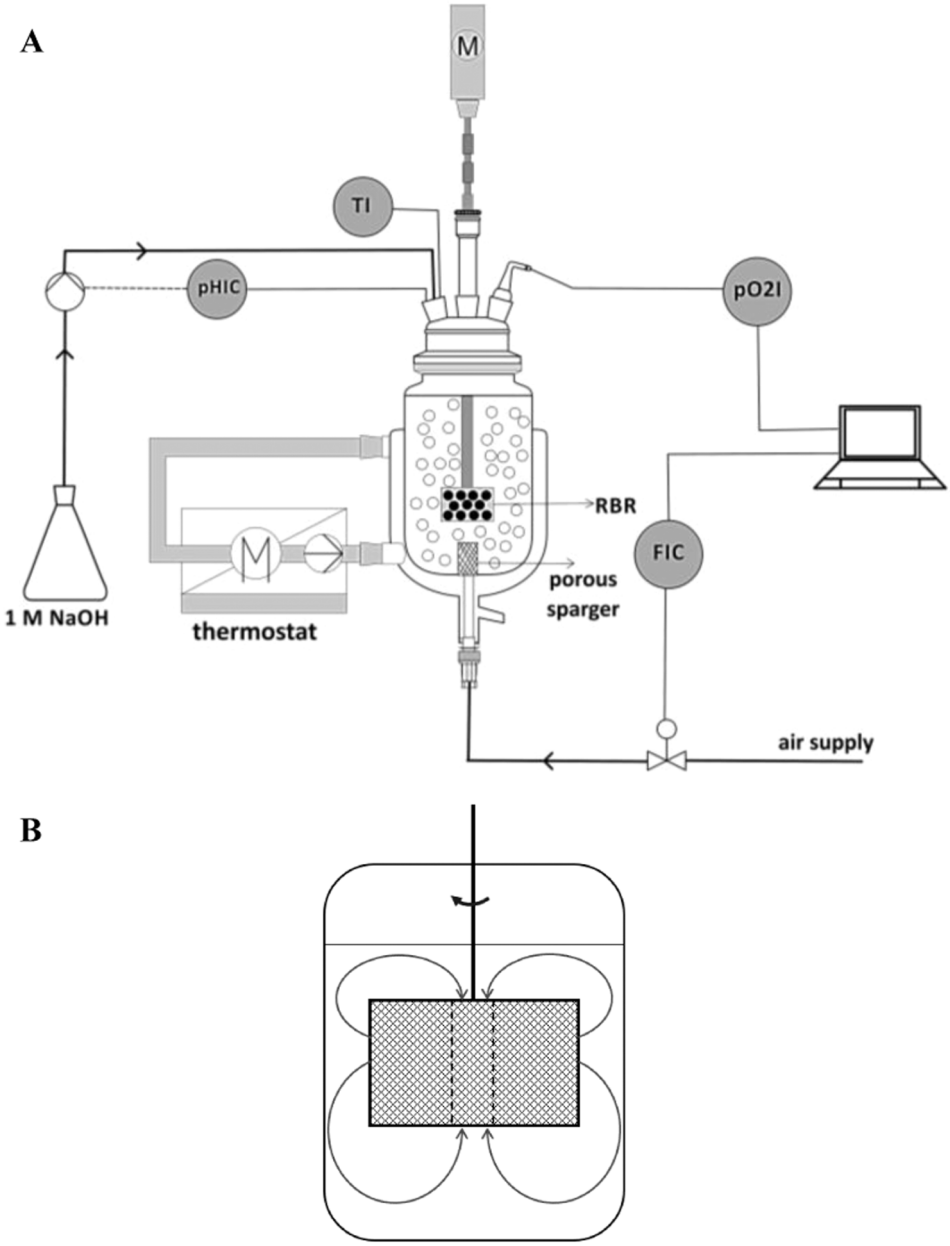

Fig. 1. A) Experimental set-up of an RBR integrated with 2 μm sintered frit porous sparger. The Piping and Instrumentation Diagram (PID) was drawn using HiTech Zang RI-CAD software version 2.2. B) The predicted flow pattern.

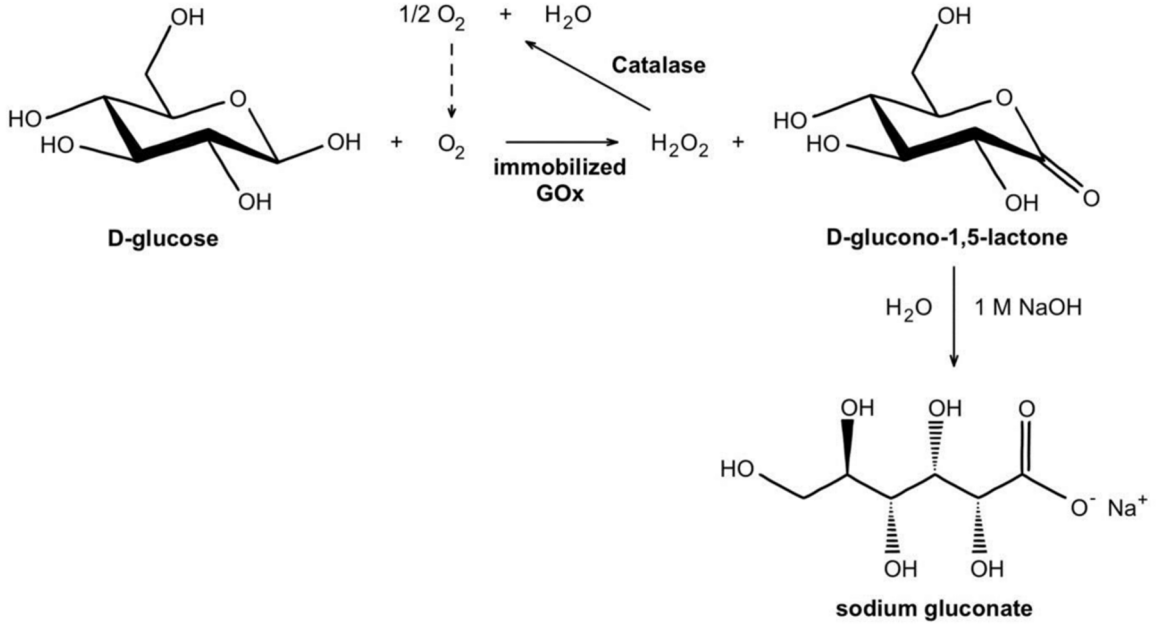

Scheme 1. Oxidation of D-glucose in D-glucono-1,5-lactone by covalently immobilized GOx on epoxy-functionalized carriers in the presence of molecular oxygen and catalase (cat).

Deutschland GmbH.

2.2. Chemicals

The substrate D-(+)-glucose, sodium acetate, acetic acid, dipotassium hydrogen phosphate (K_2HPO_4), and potassium-dihydrogen phosphate (KH_2PO_4) were purchased from Carl Roth GmbH (Germany) for the preparation of substrate and buffer solutions. Sodium hydroxide (NaOH) for inline titration and pH adjustment of solutions, o-diasidine for the enzymatic assay of GOx, and Antifoam 204 (A6426) as a surfactant (mixture of organic non-silicone polypropylene polyether dispersions) were purchased from Sigma-Aldrich/Merck (Germany). For the Bradford protein assay, Coomassie Brilliant Blue G-250 was purchased from Thermo Fisher Scientific Inc. (Germany). Sepabeads® EC-HFA and ReliZyme™ HFA 403 M grade carriers were purchased from Resindion S.r.l (Italy).

2.3. Establishment of repetitive batches with a rotating bed reactor

The SpinChem® RBR S2 and SpinChem® Vessel V2 were purchased from SpinChem AB (Sweden). The SpinChem® RBR S2 was filled with 8.2 g dried ReliZyme™ HFA 403 carriers (M grade) with immobilized GOx, using a filter (pore size 104 μm) to prevent carrier leaching. The shaft of RBR was connected to the digital overhead stirring motor IKA RW 20 Digital (Germany), which was run at 1000 rpm (see Fig. 1). The vessel V2 was connected to the thermostat Thermohaake B5 Thermoscientific (USA) to maintain a temperature of 35 °C during the course of the reaction. The compressed air was supplied to the reaction medium through the sintered frit sparger Techlab (Germany) with a pore size of 2 μm (length 2.54 cm, diameter of 1.27 cm) and an open tube sparger with an opening diameter of 2 mm. Both spargers were placed vertically at the bottom of the reactor. The distance from the top of the sintered frit sparger to the bottom of the vessel is 2.6 cm. The RBR is placed 4.1 cm from the bottom of the vessel, with a distance of 1.5 cm between the top of the sintered frit sparger and the lower end of the RBR. The compressed air flow rate was adjusted with the gas mass flow meter from Bronkhorst High-Tech B.V. (Germany).

D-glucose is oxidized to D-glucono-1,5-lactone catalyzed by the immobilized GOx in the RBR in the presence of molecular oxygen (shown in Scheme 1). Catalase (Cat) was used in its free form (the ratio of the calculated glucose oxidase activity to the calculated catalase activity was maintained above one) in solution to remove H_2O_2, which deactivates the enzyme GOx [20]. The product D-glucono-1,5-lactone dissociates to D-gluconic acid, which was titrated with 1 M NaOH by the automated titrator Titrinoplus 848 Metrohm (Switzerland) to maintain a constant pH in the reaction solution and to achieve a complete conversion by in-situ transformation of gluconic acid to sodium gluconate.

The chemical transformation of D-glucono-1,5-lactone to gluconic acid is not limited and is performed quantitatively, since the acid dissociation constant of gluconic acid (pK_a of 3.5, as calculated in the Supplementary Material) at 35 °C is lower than the value of pH 5.3 of the reaction causing deprotonation of the carboxylic acid group of gluconic acid. The titration calculation is validated on a mole basis, as one mole of NaOH consumed corresponds to one mole of gluconic acid produced. The reaction yield is determined by the ratio of a total mole of product $n_{product}$ at the end of the reaction to the initial mole of D-glucose $n_{glucose,0}$ given to the system, shown in Eq. (1).

$$\text{Yield } [\%] = \frac{n_{\text{fproduct}}}{n_{\text{glucose,0}}} \bullet 100 \quad (1)$$

2.4. Buffer selection for covalent GOx immobilization

0.07 g ReliZyme™ HFA 403 M grade carriers was incubated with 1.4 ml GOx solution (100 μg_{GOx} ml^{-1}) prepared in 100 mM potassium phosphate buffer [21] at pH 7.0 and 10 mM sodium acetate buffer at pH 5.3. The experiments were carried out at 20 rpm with the tube revolver Thermoscientific (USA) and 4 ± 1 °C for 20 h. The activity yield of immobilization was investigated by the initial rate measurements in the presence of peroxidase at 520 nm according to the glucose oxidase (GOx)/peroxidase (POD) photometric assay [23,24] from Sigma-Aldrich / Merck (Germany) at pH 5.3 and 35 °C. The unit definition of activity U ml^{-1} (μmol min^{-1} ml^{-1}) is the rate of oxidation of 1.0 μmol of β-D-glucose to D-glucono-1,5-lactone and H_2O_2 per minute. The reaction solution consisting of 0.19 mM o-diasidine, 8.84 mM D(+)-glucose and 1.93 U POD in the spectrophotometer cuvette (non-UV) was saturated with compressed air for 20 minutes to ensure oxygen saturation of the reaction solution for high GOx activity. The enzyme peroxidase oxidizes o-diasidine in the presence of hydrogen peroxide, which is a by-product

of the oxidation of glucose by the enzyme glucose oxidase in the supernatant. The photometric investigations were carried out under controlled temperature using the UV/VIS photometer Uvikon XL from Goebel Instrumentelle Analytik GmbH (Germany).

The experimental procedures for carrier drying and the equation [22] used to calculate the immobilization activity yield are shown in the Supplementary Material.

2.5. Investigation of mass transfer in a gas-liquid multiphase system

The mass transfer performance of the RBR was characterized by measuring the liquid-side volumetric mass transfer coefficient k_La (Eq. (2)) for an open tube (macrobubbles) and the 2 μm sintered frit applying the dynamic method [25,26] using compressed air and nitrogen as the stripping gas. with nitrogen as stripping gas. (The derivation of Eq. (2) is shown in the Supplementary Material.) The investigations were carried out with the RBR filled with 8.2 g dry ReliZyme™ HFA 403 M grade carriers without immobilized enzymes in 200 ml the liquid model solution (10 mM sodium acetate buffer at pH 5.3 at 35 °C). The concentration of oxygen was monitored inline with an immersed SP-PSt3-NAU-D5-YOP oxygen sensor spot connected to the Fiber Optic Oxygen Meter Fibox 4 (PreSens, Germany). The position of the sensor spot was fixed 2 mm close to the RBR and positioned 4 mm above the bottom of it for all experiments.

$$-k_La = \ln\left(\frac{c^* - c_n}{c^* - c_0}\right) \Big/ (t_n - t_0) \quad (2)$$

where the time interval $t_n - t_0$ in h is chosen in the range of 20–80% of the O_2 saturation profile to evaluate the liquid-side volumetric mass transfer coefficient k_La values

3. Results

3.1. Enzyme-carrier system

In literature [21], the buffer concentration has no effect on the activity of immobilized GOx, but it has a significant effect on the activity of free GOx. The similar activity of GOx in its free and immobilized form was achieved with 100 mM potassium phosphate buffer [21]. However, the pH of the buffer affects the activity of the immobilized GOx and the maximum value was obtained at pH 5.5 [21], which was adjusted with sodium acetate buffer. The concentration of the sodium acetate buffer was adjusted to 10 mM to avoid the effect of the salt concentration leading to the formation of less stable bubbles [27] and to minimize the bubble initial diameter, which is inversely proportional to the electrolyte concentration [28]. Furthermore, 10 mM sodium acetate buffer was sufficient to maintain the optimal pH 5.3 for performing the biocatalytic reactions at the maximum GOx activity at 35 °C in free and immobilized form [12,21]. Over 99% of the activity yield of immobilization was achieved with ReliZyme™ HFA 403 M grade carriers with 10 mM sodium acetate buffer at pH 5.3, while 51.9 ± 0.6% of the activity yield of immobilization was obtained with 100 mM potassium phosphate buffer pH 7.

3.2. Repetitive batches

ReliZyme™ HFA-type carriers are the improved form of Sepabeads as described by Resindion S.r.l. and used in many biocatalytic immobilization [29–31], on the assumption of an irreversible immobilization according to the information sheet with chemical structure and functional groups published by Resindion S.r.l. [32]. Sepabeads allow multipoint attachments according to R. Torres [33], which enhances the reuse of the biocatalyst [33–35] and no prior activation was required for covalent immobilization for Sepabeads [36]. 8.2 g dried ReliZyme™ HFA 403 M grade carriers was incubated with 90 ml of GOx solution (98 μg ml^{-1} and 685 μg ml^{-1} corresponding to the enzyme loadings of 1.07 mg_{GOx} $g^{-1}_{carrier}$ and 7.52 mg_{GOx} $g^{-1}_{carrier}$, respectively) prepared in 10 mM sodium acetate buffer at pH 5.3. The immobilization experiments were carried out at 4 ± 1 °C and 300 rpm with the shaker Edmund Bühler GmbH (Germany) for 22 hours. The supernatant was removed, and the carriers were washed with 20 ml of 10 mM sodium acetate buffer at pH 5.3 three times to wash out the unbound GOx on carriers until no change in the activity values of the wash solution was observed. After running the model reaction in the RBR under fine bubble aeration once, the RBR was washed three times with 100 ml of 10 mM sodium acetate buffer at pH 5.3 to remove any residual components, and assembled into the experimental set-up to carry out a repetitive batch.

The similar GOx specific reaction rates (4.05 U mg^{-1}_{GOx} and 3.68 U mg^{-1}_{GOx} for the validation batch 1 and batch 2, respectively, Fig. 2) were observed in the repetitive batches for the biocatalytic oxidation catalyzed by immobilized GOx and no enzyme leaching from the carriers into the reaction medium was quantified by the GOx activity measurement. This result indicates that the covalent immobilization of GOx was carried out successfully that the enzyme is not leached out, allowing the validation of the repetitive batches with the reuse of biocatalysts. In addition, the particle size range was quantified with 98.5% of carriers being in the range of 200–500 μm (shown in Fig. S2 in the Supplementary Material). No carrier leaching was detected throughout the RBR.

3.3. Enzyme loading on carriers and enzyme leaching

Immobilization allows a higher catalyst concentration in the specific reaction volume. To determine the maximum achievable enzyme loading on the ReliZyme™ HFA 403 carriers, the carriers were incubated with five different concentrated enzyme solutions (1.67, 3.35, 6.71, 12.7 and 25.5 mg_{enzyme} $g^{-1}_{carrier}$) and the initial enzyme-specific activity (0.08 ± 0.01, 0.15 ± 0.02, 0.34 ± 0.05, 0.40 ± 0.02 and 1.11 ± 0.16 U $mg^{-1)}_{carrier}$ was measured with the initial rate measurements as shown on the x-axis of Fig. 3. The residual activity in the supernatant at the end of the immobilisation was then measured and shown on the y-axis of Fig. 3. It was shown that even with a high enzyme loading of 25.5 mg_{enzyme} gc^{-1}_{arrier} on carriers, 98% of the activity yield was achieved (Fig. 3).

This result is consistent with the findings of L. Hilterhaus [37], that the saturation enzyme loading capacity for Sepabeads® EC carriers for Cal B and endoglucanase is above 100 mg_{enzyme} $g^{-1}_{carrier}$ that a higher GOx

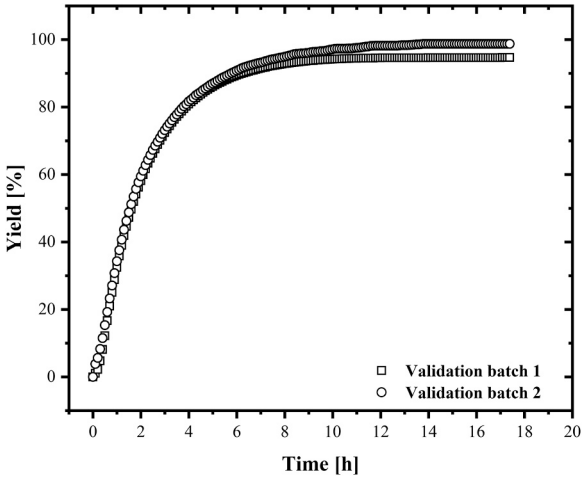

Fig. 2. Validation of repetitive batches under fine bubble aeration. 8.2 g immobilized carriers, 1000 rpm, 35 ± 1 °C, enzyme loading on carriers: 1.07 mg_{GOx} $g^{-1}_{carrier}$, calculated activity of catalase/calculated activity of GOx:1.38, 25 mM glucose solution in 10 mM sodium acetate buffer at a pH of 5.5 ± 0.2, initial volume 200 ml, 1 vvm. Catalase is used in its free form.

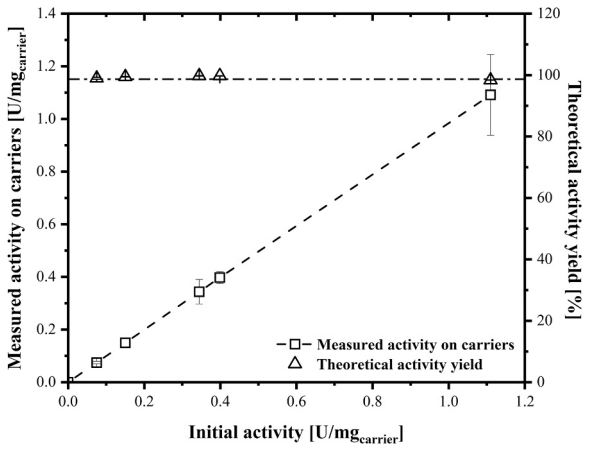

Fig. 3. Investigation of the maximum achievable immobilization capacity for ReliZyme™ HFA 403 M grade carriers (square) and the activity yield for each data point (triangle). 0.07 g carriers, 20 rpm, 4 ± 1 °C, 10 mM sodium acetate buffer pH 5.3, volume of immobilization: 1.4 ml. Carriers were incubated for 20 h.

loading could be applied on the carriers, since the saturation capacity of the carriers was not reached until the enzyme loading of 25.5 mg_{enzyme} $g_{carrier}^{-1}$.

To determine the effect of enzyme concentration on the enzyme-specific reaction rate measured with the rotating bed reactor, two different enzyme loadings on carriers as 1.07 mg_{GOx} $g_{carrier}^{-1}$ and 7.52 mg_{GOx} $g_{carrier}^{-1}$ were prepared.

Over 98% of the activity yield of immobilization was measured for both enzyme loadings with the initial rate measurements (shown in Table 1) before carrying out the biocatalytic oxidation in the rotating bed reactor. The residual activity in the supernatant after 22 h is less than 0.07 U ml^{-1} and the activity of GOx in the washing solutions for both enzyme loadings was determined to be 0.018 ± 0.003 U ml^{-1} and 0.04 ± 0.02 U ml^{-1}, respectively). No significant enzyme leaching was detected at two various enzyme loadings after each washing process.

A GOx loading greater than 7.52 mg_{enzyme} $g_{carrier}^{-1}$ was not used during the biocatalytic oxidation to investigate the effect of enzyme concentration on the reaction rate, as a 7-fold increase in enzyme concentration does not significantly improve the reaction rate at the substrate concentration of 25 mM, because a 1.1-fold increase in reaction rate was observed (see Table 2).

Table 2
Summary of the reaction rates for fine bubble and macrobubble aeration[a].

Aeration rate vvm	Enzyme amount on carriers mg_{GOx} $g_{carrier}^{-1}$	Glucose concentration mM	Reaction rate measured µmol min^{-1}	GOx-specific activity measured U mg_{GOx}^{-1}
Macrobubble aeration				
1	1.07	25	24.2 ± 0.6 R^2 = 0.9962	2.81 ± 0.07
1	7.52	600	28.5 ± 2.4 R^2 = 0.9999	0.46 ± 0.04
Fine bubble aeration				
0.125	1.07	25	23.5 ± 4.4 R^2 = 0.9994	2.74 ± 0.50
1	1.07	25	38.9 ± 9.1 R^2 = 0.9997	4.45 ± 1.04
1	7.52	25	43.7 ± 7.8 R^2 = 0.9999	0.72 ± 0.13
1	7.52	300	237 ± 50 R^2 = 0.9987	3.88 ± 0.82
1	7.52	600	368 ± 14 R^2 = 0.9739	5.82 ± 0.23

[a] 8.2 g immobilized carriers, 35 °C ± 1 °C, calculated activity of catalase/ calculated activity of GOx: 1.38 for the enzyme loading of 1.07 mg_{GOx} $g_{carrier}^{-1}$, calculated activity of catalase/ calculated activity of GOx: 1.70 for the enzyme loading of 7.52 mg_{GOx} $g_{carrier}^{-1}$ (0.28 ± 0.06 mg ml^{-1}. Antifoam 204 was used for higher enzyme concentration), 1000 rpm, 10 mM sodium acetate buffer at pH 5.5 ± 0.2, initial volume before titration 200 ml. Data fitting was applied by the Origin 2019b software for linear regression.

3.4. Comparison of the mass transfer performance of 2 µm sintered frit and open tube sparger

Since the process engineering parameters are often presented as a function of stirring rate in many studies [38–40], the first approach is to determine the influence of the stirring rate on the mass transfer performance under macrobubble aeration to ensure efficient mixing and the turbulent flow regime (Re > 4000) by means of the Reynolds Number [41,42]. H. K. Larsson [43] states that it is critical to define the Reynolds number in Equation S7 for SpinChem® RBR S221 (diameter 45.5 mm) due to its complex geometry and has chosen the impeller Reynolds number as it is used as an impeller to provide mixing in the liquid reaction medium as a single phase.

The stirring rate of 500 rpm Re = 2.3 × 10^5) and 1000 rpm Re = 4.7 × 10^5) ensure efficient mixing with a fully turbulent regime according to H. K. Larsson [43]. However, the Reynolds number

Table 1
Overview of GOx immobilization on the carriers Resindion ReliZyme™ and literature comparison.

Carrier type	GOx in the supernatant µg_{GOx} ml^{-1}	Batch	Prior to Immobilization U ml^{-1}	After Immobilization U ml^{-1}	Theoretical activity yield %	Theoretical initial activity measured U $mg_{carrier}^{-1}$	Applied enzyme loading on carriers mg_{GOx} $g_{carrier}^{-1}$
ReliZyme™ HFA 403/ GOx	98[a]	1	3.02 ± 0.13	0.035 ± 0.008	> 98	0.038 ± 0.004	1.07
		2	3.51 ± 0.13	0.018 ± 0.001	> 99		
		3	3.74 ± 0.05	0.007 ± 0.001			
	685[a]	1	33.7 ± 0.9	0.03 ± 0.01	> 99	0.34 ± 0.03	7.52
		2	29.9 ± 1.2	0.06 ± 0.01			
		3	28.7 ± 4	0.061 ± 0.006			
	1272[b]	1	62.2 ± 4.9	1.08 ± 0.76	> 98	1.11 ± 0.16	25.5
		2	48.8 ± 0.9	0.83 ± 0.01			
					Bound enzyme %		
Sepabeads EC/CALB [37]	-	-			100	-	20
	69000				85		139
Sepabeads EC/ endoglucanase [37]	2400				94		20

[a] 8.2 g immobilized carriers, 300 rpm, 4 ± 1 °C, 10 mM sodium acetate buffer pH = 5.3, volume of immobilization: 90 ml, 22 h, experiments were performed in triplicate, all investigations and the measurement of the samples were performed in triplicate.

[b] 0.07 g immobilized carriers, 20 rpm, 4 ± 1 °C, 10 mM sodium acetate buffer pH = 5.3, volume of immobilization: 1.4 ml, 20 h, experiments were performed in duplicate due to the need for high enzyme concentration.

characterization of the RBR for two-phase flow is subject to further investigation due to its complex design. In addition, the formulation of the Reynolds number depends on the physical parameters [43] such as viscosity and density of the continuous phase, as shown in Equation S7 in the Supplementary Material, as well as whether it is single-phase or biphasic [44]. The value of the liquid-side volumetric mass transfer coefficient k_La was doubled by increasing the stirring rate from 500 rpm ($13.1 \pm 0.5\ h^{-1}$) to 1000 rpm ($22.5 \pm 0.3\ h^{-1}$) for the open tube sparger and the increasing trend with the stirring rate was observed in other studies performed with rotating bed reactors in different configurations [45,46]. The concentration boundary layer becomes thinner while increasing the rotational rate, as described by D. Wenzel [18] for liquid-liquid extraction in an RBR. Using the same consideration for the gas-liquid system, the higher the rotational rate, the higher the mass transfer rate of gas molecules into the bulk medium.

In the previous studies [10–12], the mass transfer performance of the 2 μm sintered frit was compared to the 10 μm sintered frit and open tube sparger. Due to the higher volume-specific interfacial area, higher liquid-side volumetric mass transfer coefficients were achieved with the 2 μm sintered frit. Therefore, in this study, the mass transfer performance (see Fig. 4) of an open tube sparger was compared to the 2 μm sintered frit at 1000 rpm at the aeration rates ranging from 0.125 to 1 vvm. The given results are in good agreement with literature as the liquid-side volumetric mass transfer coefficient k_La is increased about 3-fold when using the 2 μm sintered frit as an aerator at a volume-specific aeration rate of 1 vvm. Furthermore, as expected, the liquid-side volumetric mass transfer coefficient depends on the aeration rate and increases with higher aeration rates [12,20,23,47,48]. All measurements were performed five times.

For the best mass transfer performance and according to T. Pedersen [49], the stirring rate 1000 rpm and the volume-specific aeration rate of 1 vvm are chosen for the investigation of the biocatalytic oxidation process. The investigation of the liquid-side volumetric mass transfer coefficient k_La is a key factor to explain the reason for achieving higher reaction rates with fine bubble aeration in the RBR at the same aeration rate and to establish similar reaction rates when using both aerators. However, it is necessary to determine first the required enzyme and substrate concentrations to carry out the reaction at the maximum achievable reaction rate at the zero-order kinetics.

3.5. Investigation of the effect of enzyme and substrate concentrations on the enzyme-specific reaction rate

The enzyme-specific reaction rate depends on the availability of dissolved oxygen in the reaction medium, which is the limiting step for biocatalytic oxidation reactions [8]. Oxygen is consumed as the second substrate (Scheme 1) in the rate Eq. (3) [50], and its availability depends on the oxygen transfer rate characterized by the parameter k_La, Eq. (2), depending on the volume-specific aeration rate.

$$\nu_R = \frac{v_{max} \bullet c_{glucose} \bullet c_{O_2}}{K_{m,glucose} \bullet c_{O_2} + K_{m,O_2} \bullet c_{glucose} + c_{glucose} \bullet c_{O_2}} \quad (3)$$

where ν_{max} in μmol min^{-1} mg_{enzyme}^{-1} is the enzyme-specific reaction rate, $c_{glucose}$ in mM and c_{O_2} in mM are the glucose and oxygen concentrations and K_m in mM is the Michaelis-Menten constant.

$$OCR = \frac{dc}{dt} = \nu_R \bullet c_{enzyme} \quad (4)$$

where oxygen consumption rate (*OCR* in mM min^{-1}) is modeled as the design equation of the batch operation [51] by the multiplication of ν_R with the enzyme concentration c_{enzyme} in mg_{enzyme} ml^{-1}.

Eq. 3 indicates that the reaction rate depends on the reactant concentrations, and that the enzyme concentration is the key parameter affecting the oxygen consumption rate (Eq. 4). To understand which parameter has the highest influence on the reaction rate, the effect of the aeration rate, enzyme concentration and substrate concentration was investigated by running the model reaction in the RBR with the 2 μm sintered frit.

The effect of the aeration rate was investigated at two different aeration rates (0.125 vvm and 1 vvm). The enzyme-specific reaction rate was measured as 23.5 ± 4.4 μmol min^{-1} ($k_La = 18.9 \pm 1.2\ h^{-1}$) at 0.125 vvm, whereas 38.9 ± 9.1 μmol min^{-1} ($k_La = 67.3 \pm 3.7\ h^{-1}$) was achieved at 1 vvm. The reaction rate is improved by 1.66 times when the volumetric mass transfer coefficient k_La was tripled under conditions where the aeration rate is increased by 8 times. The volumetric mass transfer coefficients k_La were measured in the designed liquid medium of 10 mM sodium acetate buffer at pH 5.3 (shown in Fig. 4). The improvement is not significant, since 8 times more gas has to be introduced into the system to increase the reaction rate by only 1.66 times. This finding leads to the investigation of oxygen consumption during the course of the reaction (shown in Fig. 5) at 1 vvm. It was observed that the change in oxygen concentration per time decreased at the beginning of the reaction, however, the oxygen concentration immediately increased and reached nearly the saturation point during the course of the reaction, indicating that the oxygen transfer rate is higher than the reaction rate under the given experimental conditions at 1 vvm and 25 mM substrate concentration.

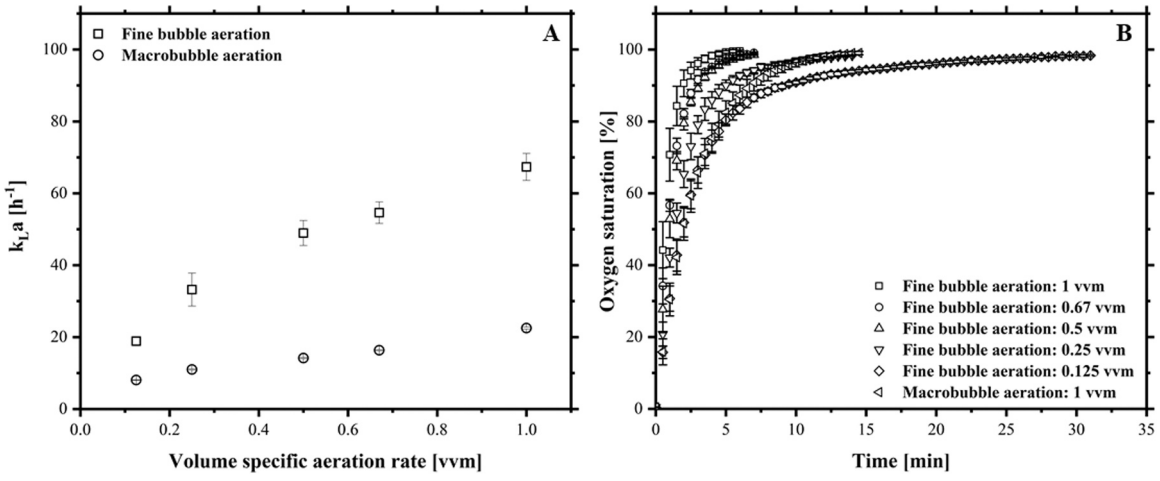

Fig. 4. Mass transfer performance for fine bubble and macrobubble aeration. A) Comparison of the volumetric mass transfer coefficients k_La for macrobubble and fine bubble aeration. B) The dynamic measurement of the time-resolved concentration curve. 8.2 g carriers, 1000 rpm, 35 ± 1°C, 10 mM sodium acetate buffer pH 5.3, volume of liquid 200 ml.

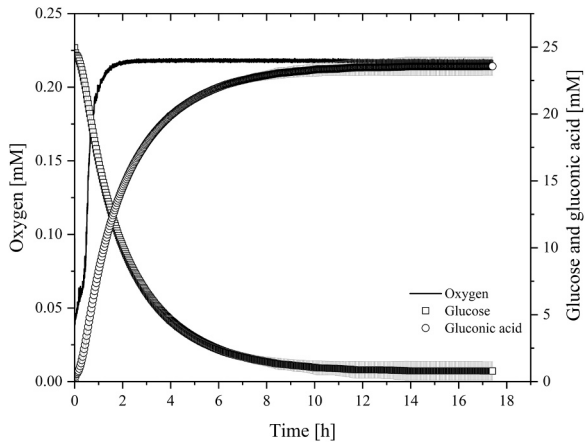

Fig. 5. Progress curve analysis of the biocatalytic oxidation of glucose in the rotating bed reactor under fine bubble aeration. 8.2 g immobilized carriers, 1000 rpm, 35 ± 1 °C, enzyme loading on carriers: 1.07 mg_{GOx} $g^{-1}_{carrier}$, calculated activity of catalase/calculated activity of GOx:1.38, 25 mM glucose solution in 10 mM sodium acetate buffer at a pH of 5.5 ± 0.2, initial volume 200 ml, 1 vvm. Catalase is used in its free form.

This raises the question of other limiting factors that could potentially affect biocatalytic performance in the rotating bed reactor. As the enzyme concentration is the key parameter influencing the oxygen consumption rate by the enzyme glucose oxidase, the biocatalytic reaction was performed with two enzyme loadings at 1 vvm at 25 mM substrate concentration.

It was shown that the reaction rate is not limited by the enzyme concentration at a substrate concentration of 25 mM (38.9 ± 9.1 μmol min^{-1} for 1.07 mg_{GOx} $g^{-1}_{carrier}$ and 43.7 ± 7.8 μmol min^{-1} for 7.52 mg_{GOx} $g^{-1}_{carrier}$) The improvement is not significant when the enzyme loading is increased by a factor of 7, as the reaction rate was shown to be substrate-dependent.

A 12- and 24-fold increase in the substrate concentration leads to a 5.42- (237 ± 50 μmol min^{-1}) and 8.42-fold (368 ± 14 μmol min^{-1}) enhancement in the reaction rate (Table 2). Therefore, the substrate concentration was depicted as the dominant parameter on the enzyme-specific reaction rate. Consequently, the performance of 2 μm sintered frit was compared with the open tube sparger under identical reaction conditions (shown in Fig. 6). The enzyme-specific reaction rate was measured as 5.82 ± 0.23 U mg^{-1}_{GOx}, (k_La = 67.3 ± 3.7 h^{-1} shown in Fig. 4) by the oxidation of 600 mM D-glucose under fine bubble aeration at 1 vvm, whereas 0.46 ± 0.04 U mg^{-1}_{GOx} (k_La = 22.5 ± 0.3 h^{-1} shown in Fig. 4) was achieved by macrobubble aeration under identical conditions (Fig. 6 and Table 2). Taking advantage of the higher liquid-side volumetric mass-transfer coefficient k_La with the 2 μm sintered frit, the reaction rate was increased by 12.9 ± 1.6 times, and the reaction was completed in 8 hours under fine bubble aeration. In all experiments, the final yield value is above 95%, which is consistent with the results of T. Pedersen [49], who investigated the oxidation process of D-glucose by the enzyme GOx in its free form.

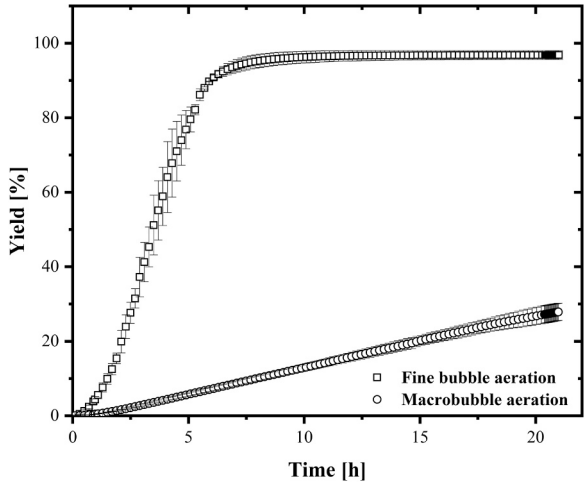

Fig. 6. The effect of the aerator type on the enzyme-specific reaction rate. 8.2 g immobilized carriers, 1000 rpm, 35 ± 1 °C, 7.52 mg_{GOx} $g^{-1}_{carrier}$, 600 mM glucose in 10 mM sodium acetate buffer pH 5.5 ± 0.2, initial volume before titration 200 ml, 1 vvm, 0.28 ± 0.06 mg ml^{-1} Antifoam 204.

The experiments were performed as duplicate. The experiments were performed in triplicate for the 2 μm sintered frit at the substrate concentration of 25 mM at 1 vvm. The duplicate experiment for the substrate concentration of 600 mM was performed with the tripled catalase activity (90,200 U), where the ratio of the calculated catalase activity to the calculated GOx activity was determined to be equivalent to 4.79. The final yield value obtained with the higher catalase concentration is the same as the result obtained with the ratio of the calculated catalase activity to the calculated GOx activity of 1.70. The similar enzyme-specific reaction rates (5.98 U mg^{-1}_{GOx} for 32,000 U and 5.66 U mg^{-1}_{GOx} for 92,000 U) were observed in the experiment, indicating that the calculated catalase activity in its free form above 32,000 U does not affect the reaction rate.

In the previous study [12], it was revealed that the gas utility for the same model reaction catalyzed by the free-form of GOx was enhanced by a factor of 25 under fine bubble aeration in a stirred tank reactor by performing the reaction at the same liquid-side volumetric mass transfer coefficient k_La at 160 h^{-1}. A similar approach was applied to demonstrate the applicability of fine bubble aeration for immobilized GOx in the RBR by establishing comparable GOx-specific-reaction rates (open tube sparger: 2.81 ± 0.07 U mg^{-1}_{GOx}, k_La = 22.5 ± 0.3 h^{-1} and 2 μm sintered frit: 2.74 ± 0.5 U mg^{-1}_{GOx}, k_La = 18.9 ± 1.2 h^{-1} at the similar mass transfer rates, where the gas consumption was reduced 8 times (1 vvm for open tube and 0.125 vvm for 2 μm sintered frit) at the substrate concentration of 25 mM. The experiments were performed as duplicate. On the basis of the statistical analysis using the ANOVA method we did not find any significant variation between the final values of the yield for all biotransformation reactions with a confidence level of 95% ($p = 0.13 > 0.05$).

3.6. Process considerations

For an economically acceptable biocatalytic process, the success factors (product concentration, catalyst productivity, and yield) were published by P. Tufvesson [52,53] and are calculated for this study (Table 3). After 21 hours, the final yield of 96.8 ± 1.2% (shown in Fig. 6)

Table 3
Process considerations for the biocatalytic synthesis of D-glucono-1,5-lactone by immobilized GOx in the RBR at 1 vvm and 600 mM substrate concentration.

Catalyst Productivity $g_{product}$ $g^{-1}_{immobilizedGOx}$	Yield %	Product g	Process time h	Product concentration g L^{-1}
Macrobubble aeration				
107 ± 8	27.8 ± 2.3	6.55 ± 0.27	21	28.1 ± 2
49.6 ± 3.5	12.9 ± 0.9	3.03 ± 0.11	10	14.1 ± 0.9
Fine bubble aeration				
373 ± 5	96.8 ± 1.2	22.8 ± 0.3	21	71.7 ± 0.0
371 ± 6	96.2 ± 1.6	22.7 ± 0.4	10	71.4 ± 0.2
Factors for economically acceptable biocatalytic processes applying immobilized biocatalysts [52,53]				
50–100	>90	-	-	> 50

was achieved with fine bubble aeration with 22.8 ± 0.3 g product (calculated), while with macrobubble aeration a yield of 27.8 ± 2.3% was achieved with 6.55 ± 0.27 g product (calculated). To have 100 g product as a basis, the reactor must be operated under macrobubble aeration for 13.8 days, assuming there is no loss of the activity of immobilized GOx.

In comparison, for the process under fine bubble aeration only 10 hours are required, and 22.7 ± 0.4 g (calculated) of product was produced. In addition to the increase in the reaction rate, the catalyst productivity is improved by a factor of 3.49 ± 0.25 when comparing the values obtained at the 21st hour for fine bubble aeration and macrobubble aeration based on the amount of calculated product produced with the same amount of enzyme glucose oxidase immobilized on carriers. Consequently, our study proves that the biocatalytic oxidation process under fine bubble aeration with SpinChem® RBR meets the industrial process requirements in terms of catalyst productivity/yield/product concentration, and the results are promising for further biocatalytic reactions.

4. Conclusion

This study focuses on proving the applicability of the fine bubble technology integrated into SpinChem® RBR. Compared to macrobubble aeration, the biocatalytic oxidation was significantly intensified, taking the advantage of the larger volume-specific interfacial area by fine bubbles. For the utilization of the RBR, covalent binding was applied for GOx immobilization on epoxy-functionalized carriers achieving over 98% of the theoretical activity yield of the immobilization. Repetitive batches were established and validated achieving the same GOx-specific reaction rate at 25 mM substrate concentration. The mass transfer performance tripled with fine bubble aeration by increasing the surface-to-volume ratio at the same volume-specific reaction rates. Substrate concentration was found to be the dominant parameter on the reaction rate and it was found that the enzyme concentration does not limit the reaction rate under the given conditions. Using the advantages of fine bubble aeration in combination with this novel reactor configuration, a glucose concentration of 600 mM was oxidized in 10 hours. The reaction rate is 12.9 ± 1.6 times higher with fine bubble aeration compared to macrobubble aeration resulting in 3.49 ± 0.25 times higher catalyst productivity with effective energy utilization due to the reduced process time. Gas consumption was reduced by 87.5% to produce the same amount of product. Therefore, this study is an example for the efficient utilization of oxidases suffering from the limitation of oxygen availability. Strategies to intensify the catalytic oxidations include increasing the surface-to-volume ratio through tubular reactors, which are limited by the scale-up of the process. In addition, operating the bioreactor under high pressure raises the oxygen solubility, allowing for higher reaction rates, however, there are challenges in establishing the process on a laboratory and larger scale. With the superiority of fine bubbles over macrobubble aeration and the advantage of using a novel reactor concept, the biocatalytic oxidation is intensified, addressing the bioprocess sustainability and bringing the fundamental knowledge [10–12, 23] of fine bubbles into practice by overcoming the limitations described.

CRediT authorship contribution statement

Zeynep Perçin: Writing – original draft & editing, Visualization, Validation, Methodology, Investigation, Data curation, Conceptualization. **Lotta Kursula:** Writing – review & editing. **Erik Löfgren:** Writing – review & editing. **Emil Byström:** Writing – review & editing. **Felix Kexel:** Writing – review & editing. **Paul Bubenheim:** Writing – review & editing, Supervision. **Michael Schlüter:** Writing – review & editing, Supervision, Resources, Project administration, Funding acquisition. **Andreas Liese:** Writing – review & editing, Supervision, Resources, Project administration, Funding acquisition.

Declaration of Competing Interest

The authors declare that they have no known competing financial interests or personal relationships that could have appeared to influence the work reported in this paper.

Data Availability

Data will be made available on request.

Acknowledgement

This work was funded by the Deutsche Forschungsgemeinschaft (DFG, German Research Foundation) – [501131738]. We want to thank our laboratory trainees, Lea Portand, Vincent Heineken, M.Sc. student Madhava Madhusoodhanan, M.Sc. student Mansi Aliveli, and B.Sc. Mona Helene Brecht for their good and reliable work in the laboratory. We would like to thank M.Sc. Mauricio Vaca Guerra for helping us measure the particle size distribution of the carriers.

Appendix A. Supporting information

Supplementary data associated with this article can be found in the online version at doi:10.1016/j.bej.2024.109333.

References

[1] S. Wu, R. Snajdrova, J.C. Moore, K. Baldenius, U.T. Bornscheuer, Biocatalysis: enzymatic synthesis for industrial applications, Angew. Chem. Int. Ed. 60 (2021) 88–119, https://doi.org/10.1002/anie.202006648.
[2] (a) J.M. Woodley Erdem, Industrially useful enzymology: translating biocatalysis from laboratory to process, Chem. Catal. 2 (2022) 2499–2505, https://doi.org/10.1016/j.checat.2022.09.037;
(b) P.W. Bridgman, The coagulation of albumen by pressure, J. Biol. Chem. 19 (1914) 511–512.
[3] G.A. Truesdale, A. Downing, Solubility of oxygen in water, Nature 173 (1954) 1236.
[4] D. Gomes, J.M. Woodley, Considerations when measuring biocatalyst performance, Molecules 24 (2019) 3573, https://doi.org/10.3390/molecules24193573.
[5] A. Al-Shameri, L. Schmermund, V. Sieber, Engineering approaches for O2-dependent enzymes, Curr. Opin. Green. Sustain. Chem. 40 (2023) 100733, https://doi.org/10.1016/j.cogsc.2022.100733.
[6] B.O. Burek, A.W.H. Dawood, F. Hollmann, A. Liese, D. Holtmann, Process Intensification as Game Changer in Enzyme Catalysis, Front. Catal. 2 (2022) 858706, https://doi.org/10.3389/fctls.2022.858706.
[7] M. Crotti, M.S. Robescu, J.M. Bolivar, D. Ubiali, L. Wilson, M.L. Contente, What's new in flow biocatalysis? A snapshot of 2020–2022, Front. Catal. 3 (2023) 1154452, https://doi.org/10.3389/fctls.2023.1154452.
[8] M.R. Chapman, S.C. Cosgrove, N.J. Turner, N. Kapur, A.J. Blacker, Highly productive oxidative biocatalysis in continuous flow by enhancing the aqueous equilibrium solubility of oxygen, Angew. Chem. Int. Ed. 57 (2018) 10535–10539, https://doi.org/10.1002/anie.201803675.
[9] J.M. Bolivar, A. Mannsberger, M.S. Thomsen, G. Tekautz, B. Nidetzky, Process intensification for O2-dependent enzymatic transformations in continuous single-phase pressurized flow, Biotechnol. Bioeng. 116 (2019) 503–514, https://doi.org/10.1002/bit.26886.
[10] D. Ohde, B. Thomas, S. Matthes, Z. Percin, C. Engelmann, P. Bubenheim, K. Terasaka, M. Schlüter, A. Liese, Fine bubble-based CO2 capture mediated by triethanolamine coupled to whole cell biotransformation, Chem. Ing. Tech. 91 (2019) 1822–1826, https://doi.org/10.1002/cite.201900113.
[11] S. Matthes, B. Thomas, D. Ohde, M. Hoffmann, P. Bubenheim, A. Liese, S. Tanaka, K. Terasaka, M. Schlueter, Hydrodynamic and mass transfer correlation in a microbubble aerated stirred tank reactor, J. Chem. Eng. Jpn. / Jcej. 53 (2020) 577–584, https://doi.org/10.1252/jcej.19we181.
[12] B. Thomas, D. Ohde, S. Matthes, C. Engelmann, P. Bubenheim, K. Terasaka, M. Schlüter, A. Liese, Comparative investigation of fine bubble and macrobubble aeration on gas utility and biotransformation productivity, Biotechnol. Bioeng. 118 (2021) 130–141, https://doi.org/10.1002/bit.27556.
[13] ISO 20480-1:2017(E): Fine bubble technology — General principles for usage and measurement of fine bubbles — Part 1: Terminology, ISO Copyright office, 2017.
[14] M. Alheshibri, J. Qian, M. Jehannin, V.S.J. Craig, A history of nanobubbles, Langmuir 32 (2016) 11086–11100, https://doi.org/10.1021/acs.langmuir.6b02489.
[15] W. Zimmerman, V. Tesar, S. Butler, H. Bandulasena, Microbubble Generation, Recent Pat. Eng. 2 (2008), https://doi.org/10.2174/187221208783478598.
[16] H. Warmeling, A. Behr, A.J. Vorholt, Jet loop reactors as a versatile reactor set up - Intensifying catalytic reactions: A review, Chem. Eng. Sci. 149 (2016) 229–248, https://doi.org/10.1016/j.ces.2016.04.032.

[17] S. Illner, C. Hofmann, P. Löb, U. Kragl, A falling-film microreactorfor enzymatic oxidation of glucose, ChemCatChem 6 (2014) 1748–1754, https://doi.org/10.1002/cctc.201400028.
[18] D. Wenzel, Rotating packed bed in liquid-liquid and liquid-solid separation, in: M. Skiborowski, A. Górak (Eds.), Process Intensification by Rotating Packed Beds, Walter de Gruyter GmbH, Berlin/Boston, 2022, p. 43, https://doi.org/10.1515/9783110724998.
[19] K. Rodríguez Núñez, C. Bernal, J.M. Bolivar, The enzyme, the support, and the key immobilization strategy: the key findings to a desirable biocatalyst, in: M. L. Ferreira (Ed.), Biocatalyst Immobilization - Foundations and Applications, Academic Press, Elsevier, 2023, p. 2.
[20] M.P. Meissner, M. Nordblad, J.M. Woodley, Online measurement of oxygen-dependent enzyme reaction kinetics, ChemBioChem 19 (2018) 106–113, https://doi.org/10.1002/cbic.201700577.
[21] G. Ozyilmaz, S.S. Tukel, O. Alptekin, Activity and storage stability of immobilized glucose oxidase onto magnesium silicate, J. Mol. Catal. B: Enzym. 35 (2005) 154–160, https://doi.org/10.1016/j.molcatb.2005.07.001.
[22] A. Liese, Lutz Hilterhaus, Evaluation of immobilized enzymes for industrial Applications, Chem. Soc. Rev. 42 (2013) 6236–6249, https://doi.org/10.1039/C3CS35511J.
[23] B. Thomas, D. Ohde, S. Matthes, P. Bubenheim, K. Terasaka, M. Schlüter, A. Liese, Enhanced enzyme stability and gas utilization by microbubble aeration applying microporous aerators, Catal. Sci. Technol. 13 (2023) 1098–1110, https://doi.org/10.1039/D2CY01761J.
[24] R.C. Jr, J.A. Bateman, Evans, Using the Glucose Oxidase/Peroxidase Systems in Enzyme Kinetics, J. Chem. Educ. 72 (1995) A240–A241.
[25] H. Ramesh, T. Mayr, M. Hobisch, S. Borisov, I. Klimant, U. Krühne, J.M. Woodley, Measurement of oxygen transfer from air into organic solvent, J. Chem. Technol. Biotechnol. 91 (2016) 832–836, https://doi.org/10.1002/jctb.4862.
[26] F. Garcia-Ochoa, E. Gomez, Prediction of gas-liquid mass transfer coefficient in sparged stirred tank bioreactors, Biotechnol. Bioeng. 92 (2005) 761–772, https://doi.org/10.1002/bit.20638.
[27] K. Ruby, S.K. Majumder, Effect of salt on the stability of microbubbles in the presence of micro−nanoparticles: substantial adsorption in the separation of particles by flotation, Ind. Eng. Chem. Res. 58 (2019) 18881–18895, https://doi.org/10.1021/acs.iecr.9b03882.
[28] S.M. Peyghambarzadeh, A. Hatami, A. Ebrahimi, A. Fazel, Photographic study of bubble departure diameter in saturated pool boiling to electrolyte solutions, Chem. Ind. Chem. Eng. Q. 20 (2014) 143–153, https://doi.org/10.2298/CICEQ120707120P.
[29] P. Borza, I. Benea, I. Bîtcan, A. Todea, S. Muntean, F. Peter, Enzymatic degradation of Azo dyes using peroxidase immobilized onto commercial carriers with epoxy groups, Stud. Ubb Chem. LXV 1 (2020) 279–290, https://doi.org/10.24193/subbchem.2020.1.22.
[30] M. Cárdenas-Fernández, E. Khalikova, T. Korpela, C. López, G. Álvaro, Co-immobilised aspartase and transaminase for high-yield synthesis of l-phenylalanine, Biochem. Eng. J. 93 (2015) 173–178, https://doi.org/10.1016/j.bej.2014.10.010.
[31] L. Babich, A.F. Hartog, L.J.C. van Hemert, F.P.J.T. Rutjes, R. Wever, Synthesis of carbohydrates in a continuous flow reactor by immobilized phosphatase and aldolase, 5, ChemSusChem 5 (2012) 2348–2353, https://doi.org/10.1002/cssc.201200468.
[32] ReliChromTM Provisory General Documentation — Resindion S.r.l., 2024. ⟨https://www.resindion.com/relizyme.php⟩.
[33] R. Torres, C. Mateo, G. Fernández-Lorente, C. Ortiz, M. Fuentes, J.M. Palomo, J. M. Guisan, R. Fernández-Lafuente, A. Novel Heterofunctional Epoxy-Amino Sepabeads, for a New Enzyme Immobilization Protocol: Immobilization-Stabilization of â-Galactosidase from Aspergillus oryzae, Biotechnol. Prog. 19 (2003) 1056–1060, https://doi.org/10.1021/bp025771g.
[34] C. Mateo, O. Abian, G. Fernández-Lorente, J. Pedroche, R. Fernández-Lafuente, J. M. Guisan, A. Tam, M. Daminati, Epoxy sepabeads: a novel epoxy support for stabilization of industrial enzymes via very intense multipoint covalent attachment, Biotechnol. Prog. 18 (2002) 629–634, https://doi.org/10.1021/bp010171n.
[35] T. Heinks, N. Montua, M. Teune, J. Liedtke, M. Höhne, U.T. Bornscheuer, G. Fischer von Mollard, Comparison of four immobilization methods for different transaminases, Catalysts 13 (2023) 300, https://doi.org/10.3390/catal13020300.
[36] C. Garcia-Galan, A. Berenguer-Murcia, R. Fernandez-Lafuente, R.C. Rodrigues, Potential of different enzyme immobilization strategies to improve enzyme performance, Adv. Synth. Catal. 353 (2011) 2885–2904, https://doi.org/10.1002/adsc.201100534.
[37] L. Hilterhaus, B. Minow, J. Müller, M. Berheide, H. Quitmann, M. Katzer, O. Thum, G. Antranikian, A.P. Zeng, A. Liese, Practical application of different enzymes immobilized on sepabeads, Bioprocess Biosyst. Eng. 31 (2008) 163–171, https://doi.org/10.1007/s00449-008-0199-3.
[38] M. Zlokarnik, Stirring: Theory and Practice, Wiley-VCH, Weinheim, Chichester, 2001, p. 76, 83.
[39] A. Rosseburg, J. Fitschen, J. Wutz, T. Wucherpfennig, M. Schlüter, Hydrodynamic inhomogeneities in large scale stirred tanks – Influence on mixing time, Chem. Eng. Sci. 188 (2018) 208–220, https://doi.org/10.1016/j.ces.2018.05.008.
[40] B.J. Michel, S.A. Miller, Power requirements of gas-liquid agitated systems, AIChE 8 (1962) 262–266, https://doi.org/10.1002/aic.690080226.
[41] P.M. Doran, Bioprocess Engineering Principles. Waltham, Academic Press. Elsevier, 2013, p. 204.
[42] Y.A. Çengel, J.M. Cimbala, Fluid Mechanics – Fundamentals and Applications, Mc. Graw-Hill, New York, 2006, p. 324.
[43] H.K. Larsson, Modelling of mass transfer phenomena in chemical and biochemical reactor systems using computational fluid dynamics, Dan. Tek. Univ. (DTU) (2015) 166.
[44] M.C. McCray, P.G.A. Cizmas, Experimental investigation of the critical Reynolds number for bubbly two-phase flow, Incas Bull. 15 (2023) 2247–4528, https://doi.org/10.13111/2066-8201.2023.15.3.4.
[45] H.-S. Liu, C.-C. Lin, S.-C. Wu, H.-W. Hsu, Characteristics of a rotating packed bed, Ind. Eng. Chem. Res. 35 (1996) 3590–3596, https://doi.org/10.1021/ie960183r.
[46] W. Liu, Y. Luo, Y.B. Li, G.W. Chu, Scale-up of a rotating packed bed reactor with a mesh-pin rotor: (II) Mass transfer and application, Ind. Eng. Chem. Res. 59 (2020) 5124–5132, https://doi.org/10.1021/acs.iecr.9b06684.
[47] Y. Chisti, U.J. Jauregui-Haza, Oxygen transfer and mixing in mechanically agitated airlift bioreactor, Biochem. Eng. J. 10 (2002) 143–153, https://doi.org/10.1016/S1369-703X(01)00174-7.
[48] R. Petříček, T. Moucha, J.F. Rejl, L. Valenz, J. Haidl, T. Čmelíková, Gas-liquid-solid volumetric mass transfer coefficient and impeller power consumptions for industrial vessel design, Int. J. Heat. Mass Transf. 121 (2018) 653–662, https://doi.org/10.1016/j.ijheatmasstransfer.2018.01.041.
[49] A. Toftgaard Pedersen, T.M. de Carvalho, E. Sutherland, G. Rehn, R. Ashe, J. M. Woodley, Characterization of a continuous agitated cell reactor for oxygen dependent biocatalysis, Biotechnol. Bioeng. 114 (2017) 1222–1230, https://doi.org/10.1002/bit.26267.
[50] R.H. Ringborg, A.T. Pedersen, J. Woodley, Automated determination of oxygen-dependent enzyme kinetics in a tube-in-tube flow reactor, ChemCatChem 9 (2017) 3285–3288, https://doi.org/10.1002/cctc.201700811.
[51] D. Vasic-Racki, U. Kragl, A. Liese, Benefits of enzyme kinetics modelling, Chem. Biochem. Eng. Q 17 (2003) 3–14.
[52] P. Tufvesson, W. Fu, J.S. Jensen, J.M. Woodley, Process considerations for the scale-up and implementation of biocatalysis, Food Bioprod. Process. 88 (2010) 3–11, https://doi.org/10.1016/j.fbp.2010.01.003.
[53] P. Tufvesson, J. Lima-Ramos, J.S. Jensen, N. Al-Haque, W. Neto, J.M. Woodley, Process considerations for the asymmetric synthesis of chiral amines using transaminases, Biotechnol. Bioeng. 108 (2011) 1479–1493, https://doi.org/10.1002/bit.23154.